

27. *The Structure of the Earth's Crusts near
the Japan Trench, off Sanriku, and also
near the Inland Sea of Japan.*

By Seiti YAMAGUTI,

Earthquake Research Institute.

(Read Nov. 15, 1938.—Received March 20, 1939.)

The investigation into the problem of determining the subterranean mass distributions direct from the corresponding gravity anomalies observed along the earth's surface, has already been made by Chûji Tsuboi and Takato Fuchida,¹⁾ who give actual examples of the gravity anomalies near Java and near North America. In this paper, the configurations of the earth's crust near the Japan Trench, off Sanriku, as well as near the Inland Sea of Japan, were calculated by the same method. The object of our investigation was to ascertain the part of the crust in which earthquakes are most frequent.

The gravity anomalies on land near the Tôhoku Districts, near the Inland Sea of Japan, and near the Japan Trench, off Sanriku, have already been published elsewhere.^{2), 3)}

1. *Near the Japan Trench.*

Along the five north parallels of 39°, 39° 30', 40°, 40° 30', and 41°, with equal lengths of 585 km, 14 points on each (70 in all) were taken with equal intervals beginning from the coast of the Japan Sea toward the Pacific Ocean, off Sanriku, as shown, in Fig. 1, *a*.

The values of the gravity anomalies for 70 points were calculated by interpolation, and the mean values, 14 in number, for each 5 points having equal longitudes, were obtained and plotted as ordinates against the distance x , the origin of which was taken at the coast of the Japan Sea, as shown in Fig. 2, *a*. The corresponding mean values of the heights of the land and the depths of the sea bottom $\pm h$, were taken from the map and the bathymetric chart of the sea near Japan, published by the Land Survey Department of the Imperial Japanese Army, and the Hydrographic Office of the Imperial Japanese Navy,

1) C. TSUBOI and T. FUCHIDA, *Bull. Earthq. Res. Inst.*, 15 (1937); 16 (1938).

2) H. NAGAOKA, S. SHINJÔ, and R. CTANI, *Journ. Coll. Sci. Tokyo*, 16 (1902).

3) M. MATUYAMA, *I. U. Geod. Geophys.*, 6 Conf., (1935).

respectively, and plotted as ordinates against x , which in this case extends from -355 km to 585 km, as shown in Fig. 2, *d*. The negative

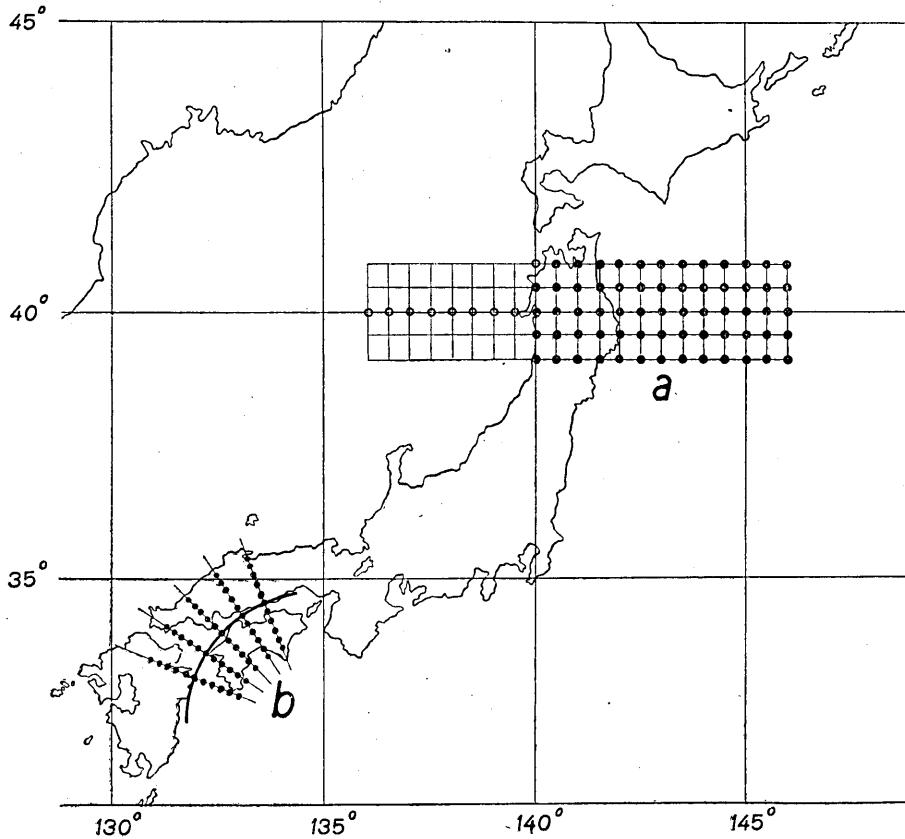


Fig. 1.

value of x means the distance from the origin just mentioned to the Japan Sea side or to the west.

The gravity anomalies used above have no corrections for the attraction of the water masses of the deep seas of the Pacific Ocean and of the Japan Sea, so that we tried to add these corrections to the gravity anomalies before calculating the subterranean mass distribution.

Let $g(y)$ be the gravity at a point P , due to the linear mass with depth h , and density ρ , which extends from $+\infty$ to $-\infty$ as shown in Fig. 3, we then have

$$g(y) = \frac{2\rho}{h}.$$

Now, the vertical section which is plotted on the same scale as h —

diagram (in Fig. 2, d) is divided by parallel lines with equal intervals

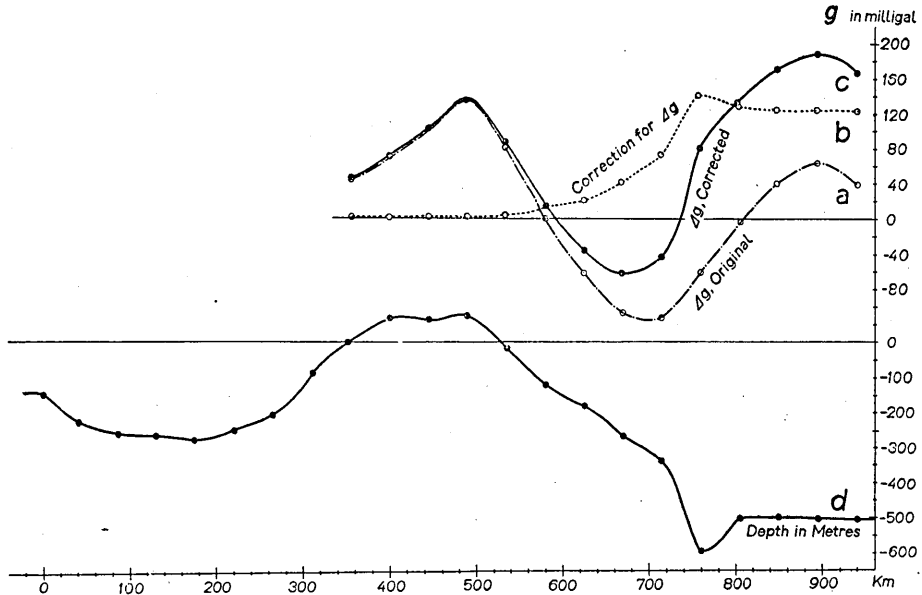


Fig. 2. Near Sanriku.

of depths, 500 metres, and also with equal distances of 20 km, namely, from $h=0$ to $h=6000$ metres and from $x=0$ to $x=460$ km, respectively. Each elementary rectangle thus divided, with the mass ρ , was assumed to be the elementary mass that affects the gravity value. The value of $g(x)$ at the origin due to each elementary mass, which is assumed to be concentrated at the centre of gravity, was calculated by the formula

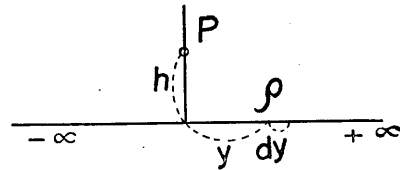


Fig. 3.

$$g(x) = \frac{k^2 2\rho}{\sqrt{x^2 + h^2}} \cdot \frac{h}{\sqrt{x^2 + h^2}} = \frac{2\rho k^2 h}{x^2 + h^2}$$

where

$$\rho = (2.7 - 1.03) \times 5 \times 10^4 \times 20 \times 10^5 = 1.67 \times 10^{11},$$

and

$$k^2 = 6.68 \times 10^{-8}$$

in absolute unit, and allotted to each rectangle. The final values of $g(x)$ at 14 points were calculated by summing the values on every

rectangle that is contained in the area between the curve of depth, h and the axis of x in Fig. 2 *d*, instead of integrating the whole submarine area, and the correction curve was plotted as shown in Fig. 2 *b*. When $x=460$ km, the value of $g(x)$ converges to zero, its sum being considered practically equal to its integrated sum.

The original curve of the gravity anomalies added to this correction curve was called the *corrected curve*, as shown in Fig. 2 *c*. From the *corrected curve*, the values for every 32.5 km, of which there are 36 in all, were read off, assuming the curve to be repeated as a symmetric image with respect to the end point, which is distant from the origin by 585 km. With these 36 values, the gravity anomalies were expanded into the series

$$\Delta g(x) = \sum_0^{18} a_n \cos nx + \sum_1^{17} b_n \sin nx.$$

The coefficients of the Fourier terms found, taking Δg in milligal, were:

Table I. The sine terms are here all zero.

n	0	1	2	3	4	5	6	7	8	9
cos	70.3	-31.2	90.7	-35.2	-47.4	3.0	-4.1	-1.6	6.2	3.7
n	10	11	12	13	14	15	16	17	18	
cos	-6.7	3.0	-2.0	-1.6	-1.5	-1.2	-1.7	2.1	0.1	

If we assume that the mass responsible for these gravity anomalies is at a depth of 15 km, which corresponds to $\frac{\pi}{39}$, then the Fourier coefficients for

$$2k^2\pi\rho(x) = \sum_0^{18} a_n e^{n\pi d} \cos nx + \sum_1^{17} b_n e^{n\pi d} \sin nx,$$

and the values of $\rho(x)$ become:

Table II a.

n	0	1	2	3	4	5	6	7	8	9
cos	70.7	-33.7	107.0	-44.7	-65.5	4.5	-6.7	-2.8	11.8	7.7
n	10	11	12	13	14	15	16	17	18	
cos	-15.0	7.0	-5.3	-4.6	-4.7	-4.0	-6.2	8.3	0.4	

With these coefficients, the summation for $\rho(x)$ was carried out, and its value divided by 0.6, which is the difference of the densities of

Table II b.

x in degree $\rho(x)$ in km	0	10	20	30	40	50	60	70	80	90
$\rho(x)$	0.95	2.38	3.40	4.33	6.81	4.88	3.00	-0.68	-1.95	-3.02
x in degree $\rho(x)$ in km	100	110	120	130	140	150	160	170	180	
$\rho(x)$	-3.82	-3.55	0.58	5.25	5.74	7.18	8.11	8.27	5.90	

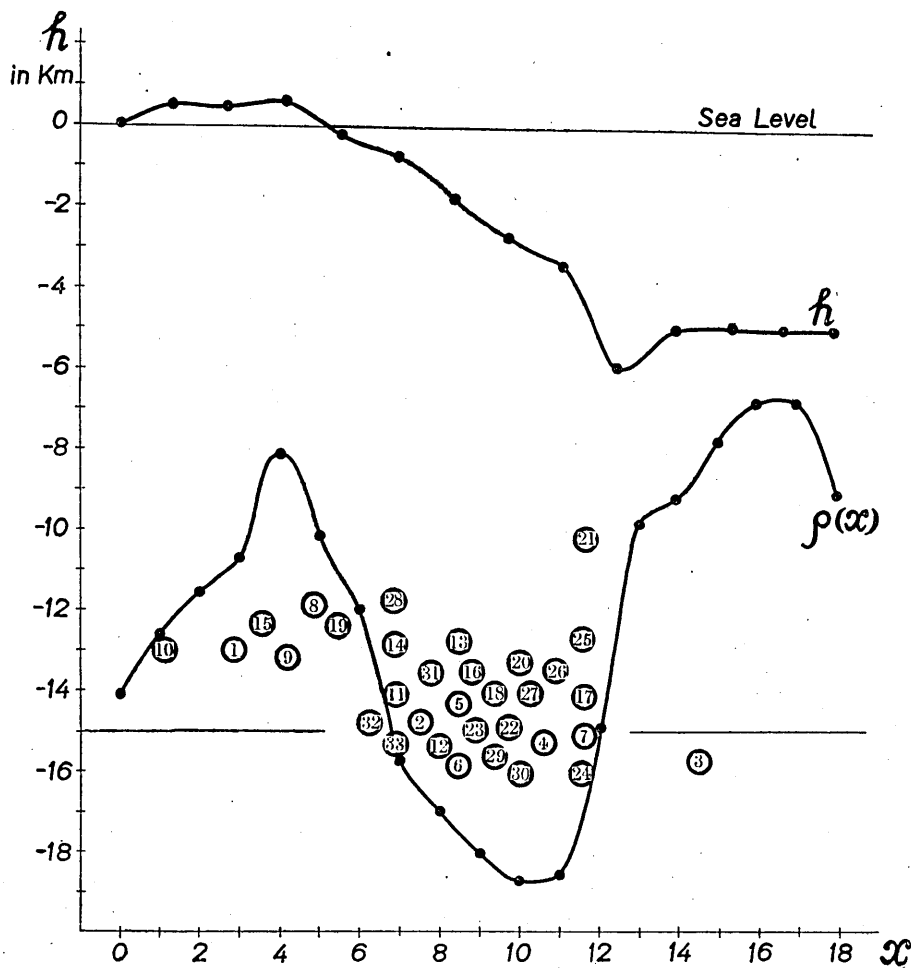


Fig. 4. Near the Japan trench, off Sanriku.

the crustal (2.7) and the subcrustal (3.3), so that they could be expressed in km, as shown in Table II b, and plotted as ordinate against the same axis of x together with the h -curve as shown in Fig. 4.

C. Tsuboi calculated the thickness of the crustal near northeastern Japan on the basis of K. Wadati's⁴⁾ observation of seismic waves for deep-focus earthquakes, as follows:

If, in Fig. 5, we let the thicknesses of the crustal near western Japan and northeastern Japan be d' and d , and the velocities of seismic waves in the crustal and subcrustal be v_1 and v_2 , respectively, then we have the following equation from Wadati's result of observations that, in northeastern Japan, the seismic waves are observed earlier than in western Japan by 1 second,

$$\frac{d'}{v_1} - \left\{ \frac{d'-d}{v_2} + \frac{d}{v_1} \right\} = 1. \quad \therefore d' - d = \frac{v_1 v_2}{v_2 - v_1}.$$

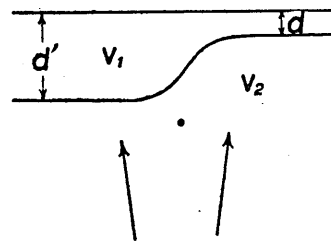


Fig. 5.

For various values of v_1 and v_2 , the values of $d' - d$ were calculated and tabulated as shown in Table III, from which we have 30 km for the probable value. Now, from investigations on the propagations of

Table III.

v_2 \ v_1	5.6	5.7	5.8	5.9	6.0 in km/sec
7.1	26	29	31	33	38
7.2	25	27	29	32	36
7.3	24	26	29	30	33
7.4	23	25	27	29	31
7.5 in km/sec	22	24	26	28	30 in km

seismic waves, the thickness of the crustal in western Japan is known to be nearly 50 km, so that we have for the thickness of the crustal in northeastern Japan, $d = 50 - 30 = 20$ km, approximately.

If we take the values of d , as explained above, to be 20 and 30 in km, then the Fourier coefficients for $2\pi k^2 \rho(x)$ and the values of $\rho(x)$ become respectively as shown in Table IV and in Fig. 6.

The hypocentres of 33 conspicuous earthquakes that occurred in the same area in Sanriku Districts as that on which the gravity anomalies were taken during a period of exactly 15 years, from Oct.

4) K. WADATI, *Geophys. Mag.*, 8 (1935) 303, 325.

1923 to Sept. 1938, were taken from the Monthly Report of the Central Meteorological Observatory in Japan, and plotted on the curve of $\rho(x)$ as shown in Fig. 4. From this diagram, we can see at a glance that

Table IV a.

n	0	1	2	3	4	5	6	7	8	9
\cos $d=20$ km	70.3	-34.6	112.5	-48.6	-72.6	5.1	-7.8	-3.4	14.6	9.7
\cos $d=30$ km	70.3	-36.8	125.1	-57.0	-90.2	6.7	-10.8	-5.0	22.6	15.9
n	10	11	12	13	14	15	16	17	18	
\cos $d=20$ km	-19.5	9.7	-7.2	-6.4	-6.7	-6.0	-9.5	13.0	0.7	
\cos $d=30$ km	-33.6	17.7	-13.8	-13.0	-14.3	-13.5	-22.4	32.5	1.8	

Table IV b.

x in degree $\rho(p)$ in km	0	10	20	30	40	50	60	70	80	90
$\rho(x)$ $d=20$ km	0.53	2.33	3.42	4.25	7.55	4.97	3.31	-1.08	-2.12	-3.32
$\rho(x)$ $d=30$ km	0.37	1.43	4.14	3.63	9.31	5.81	3.28	-1.47	-2.94	-4.04
x in degree $\rho(x)$ in km	100	110	120	130	140	150	160	170	180	
$\rho(x)$ $d=20$ km	-4.22	-4.28	0.40	5.83	5.73	7.43	8.34	8.75	5.42	
$\rho(x)$ $d=30$ km	-4.53	-7.13	1.00	6.80	5.94	8.21	8.12	11.32	3.46	

a small number of earthquakes (6 in all, about 20 percent) occurred in the subcrustal layer just beneath land, and very rarely (only one, about 3 percent) in the subterranean layer beyond the Japan trench, and that almost all the earthquakes occurred in the crustal or near the boundary of the crustal and the subcrustal on the western side of, and about, the Japan trench. The boundary curve of the crustal and the subcrustal is nearly parallel to the earth's surface and the sea bottom, or h -curve, until a certain point, 150 km off Sanriku, whence

they are in opposite phase up to the Japan trench, so that the thickness of the crustal becomes very small beyond the trench.

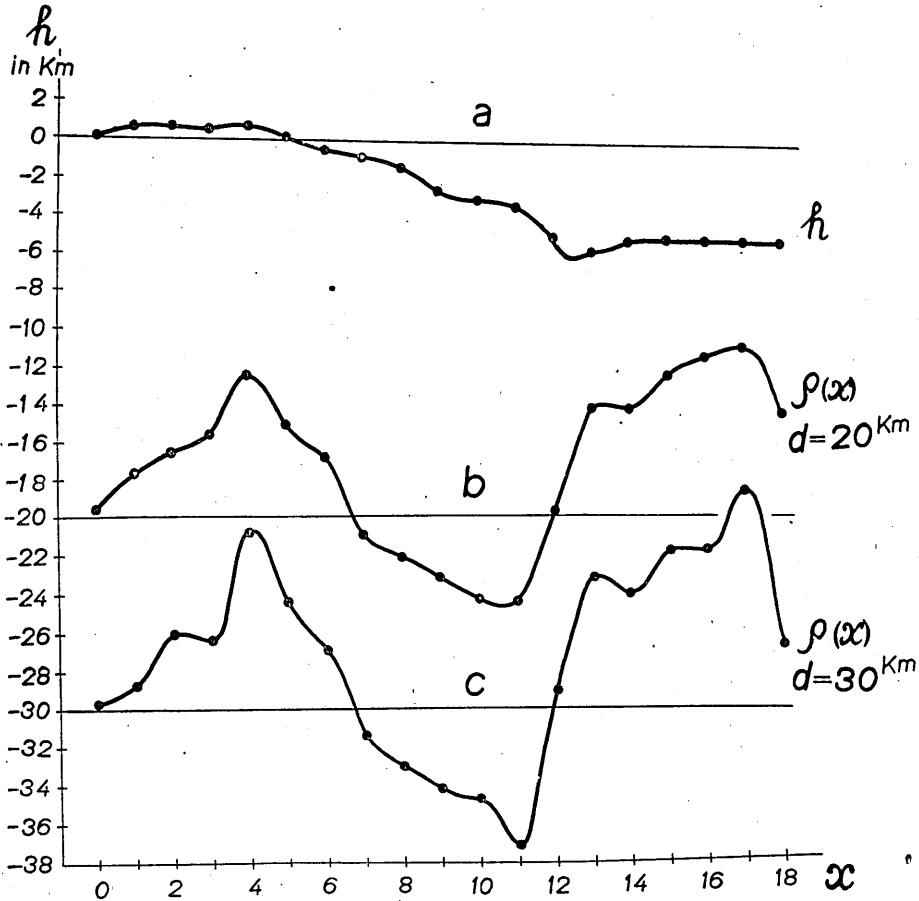


Fig. 6. Near the Japan trench, off Sanriku.

The fact that most of the conspicuous earthquakes occur in such a part of the crustal or near the boundary of the crustal and the subcrustal about the Japan trench, whichever seems to have maximum stress near it, may supply a clue to the mechanism of earthquake occurrence, the further working out of which must be reserved for a future investigations.

2. Near the Inland Sea of Japan.

We drew a curve through the eastern coast of Kyûsyû, across the Bungo Strait, through the Inland Sea, touching the coast line of the Province of Okayama. The least values of gravity anomalies lie on

this curve. To this curve, 5 orthogonal straight lines which pass through Miho and Muroto, Simane Ôta and Kôti, Hamada and Matuyama, Ube and Uwasima, Kurume and Asiduri, respectively, were drawn, as shown in Fig. 1, *b*. On each straight line, 12 points were taken with equal intervals of 20.2 km, the middle points being taken on the central curve drawn above. The values of the gravity anomalies were smoothed for each five stations lying on the curve that is parallel to the central curve, and plotted as shown in Fig. 7, *a*. With these 12 values, the gravity anomalies were subjected to harmonic analysis. The coefficients of the Fourier terms found taking Δg in milligal, were:

Table V.

n	0	1	2	3	4	5	6
sin		- 6.60	- 1.40	- 1.60	0.03	0.10	
cos	19.65	20.10	1.68	0.67	- 0.02	0.27	- 0.33

If we assume that the mass responsible for these gravity anomalies is at depths of 20, 30, and 40 km, which correspond to $\frac{\pi}{5.55}$, $\frac{\pi}{3.70}$ and $\frac{\pi}{2.78}$ respectively, then the Fourier coefficients for $2\pi k^2 \rho(x)$, taking Δg in milligal become:

Table VI.

	n	0	1	2	3	4	5	6
$d=20$ km	sin		-11.6	- 4.3	- 8.8	0.3	1.7	
	cos	19.7	35.4	5.2	3.7	- 0.2	4.6	- 9.9
$d=30$ km	sin		-15.4	- 7.6	-20.5	0.9	7.0	
	cos	19.7	47.1	9.2	8.6	- 0.6	18.9	-53.1
$d=40$ km	sin		-20.4	-13.5	-47.8	2.8	28.2	
	cos	19.7	62.3	16.2	20.0	- 1.8	76.1	-294.0

With these coefficients, the values of $\rho(x)$ were calculated and plotted as ordinates, together with the values of the heights of the land, h , against the distance x , similarly treated as in the case of Sanriku, as shown in Table VII, and Fig. 7. The values for the sea depths were multiplied by 0.62, which is the ratio of the difference of the

Table VII.

x in degree $\rho(x)$ in km		0	30	60	90	120	150	180	210	240	270	300	330	σ
		km	1.66	0.32	0.92	-0.66	-0.18	-1.15	0.64	-0.06	1.01	1.55	3.02	
$d=20$ km	$\rho(x)$	2.54	1.37	0.69	0.47	-0.13	-0.76	-0.57	0.10	0.37	0.69	1.78	2.83	$\sum_0^3 (\sin + \cos)$
	$\rho'(x)$	1.14	0.39	0.38	0.93	0.97	0.68	0.84	1.09	0.68	0.23	0.68	1.38	$a_0 + \sum_2^3 (\sin + \cos)$
	$\rho''(x)$	1.98	2.84	-1.59	2.98	-2.98	1.37	-3.95	2.87	-2.00	2.02	0.54	5.27	for all terms
$d=30$ km	$\rho(x)$	3.36	1.20	0.41	0.62	-0.26	-1.51	-1.06	0.16	0.27	0.21	1.99	3.97	$\sum_0^3 (\sin + \cos)$
	$\rho'(x)$	1.49	-0.11	-0.04	1.23	1.20	0.41	0.81	1.48	0.68	-0.40	0.52	2.04	$a_0 + \sum_2^3 (\sin + \cos)$
	$\rho''(x)$	7.65	-1.45	0.23	2.28	-2.58	2.38	-4.93	3.00	-0.35	-2.14	4.68	2.77	for all terms, except a_0
$d=40$ km	$\rho(x)$	4.70	0.48	-0.26	1.23	-0.23	-2.88	-1.84	0.80	0.26	-0.95	2.07	6.02	$\sum_0^3 (\sin + \cos)$
	$\rho'(x)$	2.22	-1.25	-0.79	2.04	1.72	-0.33	0.63	2.54	0.79	-1.76	0.13	3.54	$a_0 + \sum_2^3 (\sin + \cos)$

densities of the crustal and water to that of the crustal, and utilised as the values of h . Here, at first glance, the two curves for h and

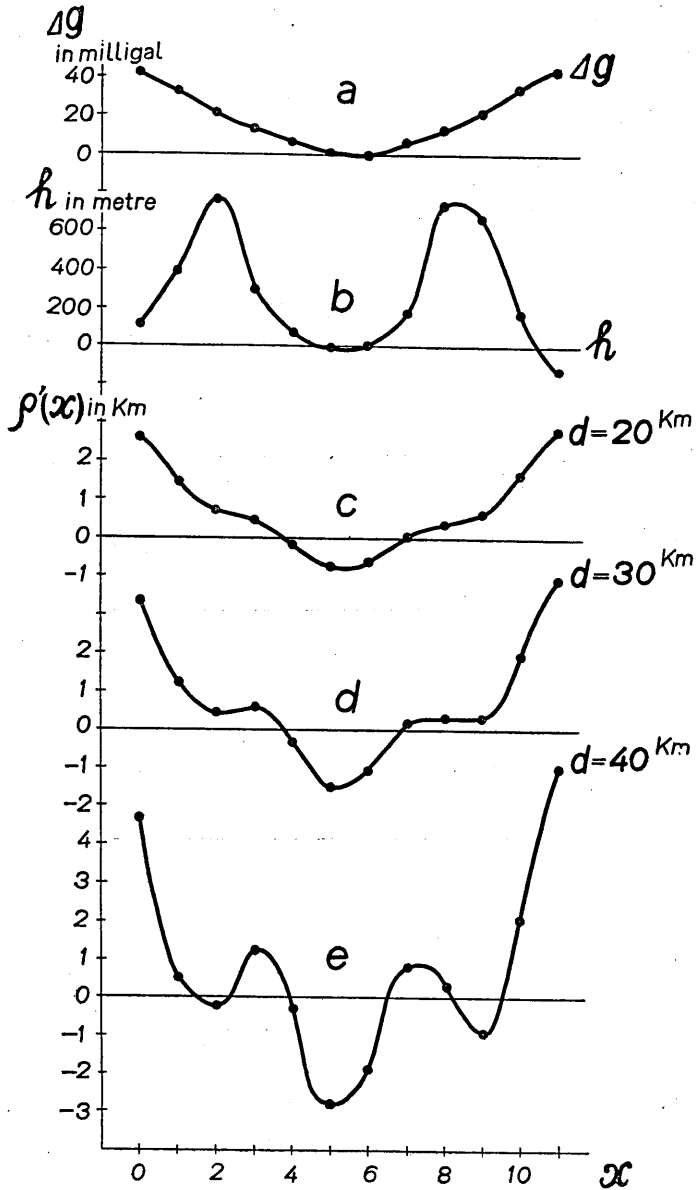


Fig. 7. $\rho'(x) = \sum_0^3 (\sin + \cos)$, near the Inland Sea.

$\rho(x)$ seem to be parallel in the first harmonics, but of opposite phase in the second harmonics, so that not only the summation for complete terms, but also the summation for the constant, the first, the second,

and the third terms, as well as for the constant, the second and the third terms, were carried out, and denoted by $\rho(x)$, $\rho'(x)$, and $\rho''(x)$, respectively. These values, thus calculated, and those of h , and Δg were plotted as shown in Figs. 7, 8. The curve of h and that of $\rho''(x)$,

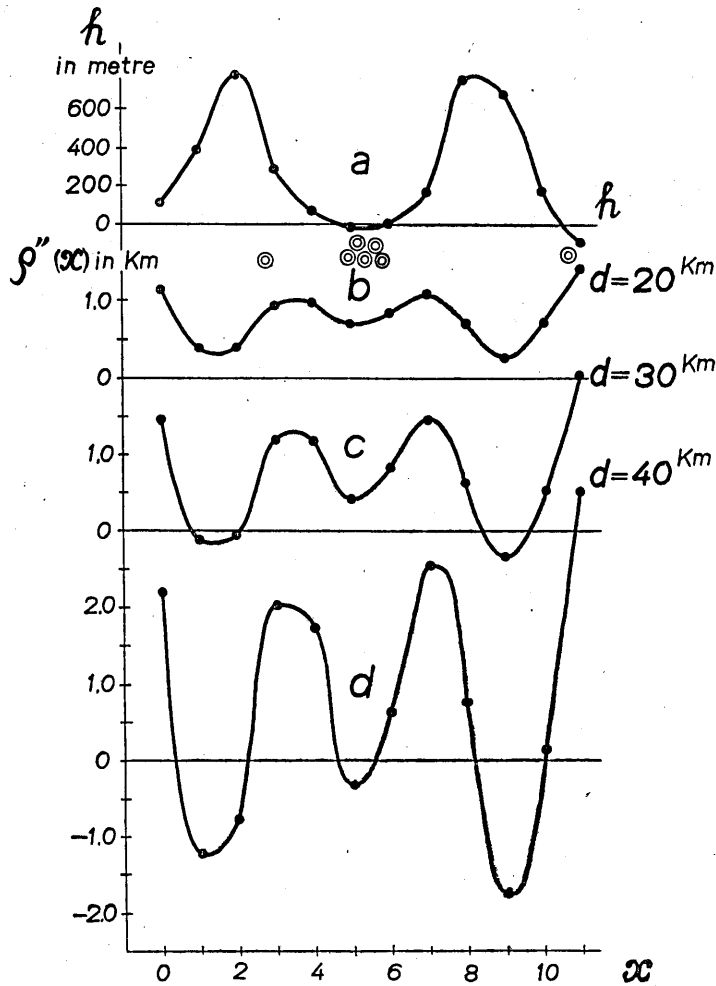


Fig. 8. $\rho''(x) = a_0 + \sum_{\frac{3}{2}}^3 (\sin + \cos)$, near the Inland Sea of Japan.

⊙: Conspicuous earthquakes.

eliminating the first harmonic terms, are rather conspicuously in opposite phase for the spaces corresponding to the lands of Tyûgoku and Sikoku.

With the values of the heights of the lands and the depths of the sea-bottoms, h , the configuration of the boundary between the crustal

and the subcrustal, was calculated, assuming that at a depth of 30 km, isostatic compensation is fulfilled.

Thus, we get $\rho_0(x) = -\frac{2.7}{0.6}h(x)$. The discrepancy of $\rho'(x)$ from $\rho_0(x)$ was also calculated and plotted against x , together with the value of $h(x)$ as shown in Fig. 9.

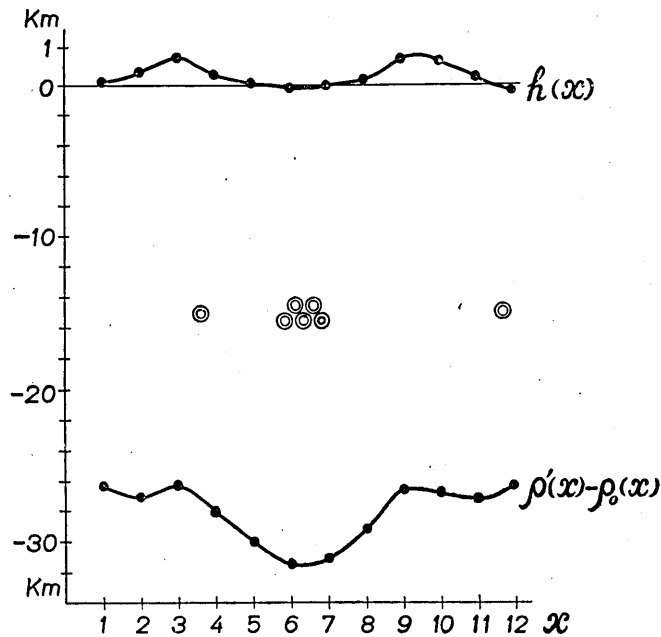


Fig. 9. $h(x)$ and $\rho'(x) - \rho_0(x)$ when $d=30$ km where $\rho_0(x) = -\frac{2.7}{0.6}h(x)$.

⊙: Conspicuous earthquakes.

The conspicuous earthquakes that occurred in the regions here investigated, during the period of 15 years from Oct. 1923 to Sept. 1938, were taken, and the approximate positions of their hypocentres plotted on the diagrams, as shown in Fig. 8 and 9. In this case, the number of earthquakes being very few (only seven), we can say nothing definite, but the fact that the five earthquakes out of the seven, occurred in the submarine area where isostatic compensation is not fulfilled, and only one occurred in the land area on which the isostatic compensation is considered to be fulfilled, as shown in Fig. 8 and 9, might provide some hints on the relation between the conspicuous earthquakes and the structure of the earth's crust. For the "rather conspicuous" earthquakes, 29 in number, also, the same relation is to be seen, i. e. the number of earthquakes that occurred in the land area forms only 30 percent

of the total. Those that occurred in the same area of submarine space formed 70 percent.

In conclusion, I wish to express my best thanks to Dr. C. Tsuboi, who has given me many useful suggestions in the course of these studies.

27. 日本海溝附近並に瀬戸内海附近の地殻構造

地震研究所 山口 生 知

坪井忠二博士の研究 방법에依つて、三陸地方日本海溝附近及び瀬戸内海附近の地殻構造を夫々の地方の地表面に於ける重力の値より計算に依つて推定する事を試みた。又地殻構造の如何なる所に於て顯著地震が最も起り易いかと云ふことも調べて見た。其の結果は次の通りである。

1. 日本海溝附近に於いては、京都帝國大學の松山教授が観測された重力異常の値に更に深海の海水の引力に依る補性を加へたものを基として、地下の質量分布を計算して見ると第四圖に示す通り、海岸から沖の方に向つて約 150 斤位迄は地表層と其下の層との境界線が略々海底の形と平行になつて下の方に下つて居り、海溝附近に近づくると海底の形と前に述べた境界線の形勢とは位相が正反對となり、更に沖の方に向つて海溝を通り過ぎると表面層は急激に薄くなつて居ることが見出される。

大正十二年十月より昭和十三年九月迄満十五ヶ年間に此の地方に起つた顯著地震の震源の大體の位置を此の鉛直断面圖に盛り込んで見ると、日本海溝附近に於いて、地表層が其の下の岩石の層の中に落ち込んで居る近傍で殆んど大部分の地震が起つて居る。而して陸地の眞下に當る場所では、約 20% の地震が起り、日本海溝を越えた沖合の地下層に於いては只の 1 個しか起つて居ない。此の著しい事實は地震發生と地下構造との關係に一つの暗示を與へるものと思はれる。

2. 瀬戸内海附近に於いては第八圖及第九圖に示す通り、中國及四國の陸地の眞下に於ける地下の質量分布の有様は、陸地の高底曲線と位相が略々正反對で、大體 Isostasy が成立つて居ると推察されるのであるが、瀬戸内海、及豊後水道等の海の眞下に於いては、地殻均衡が保たれて居らない様に見える。而して三陸地方の場合と同様に、前述の十五ヶ年間にこの地方に起つた顯著地震を盛り込んで見た。此の場合には僅かに 7 個の地震しか起つて居らないから正確なことは云はれないが、7 個の内 5 個迄が地殻均衡の保たれて居らない様に推定されることの海の領域の地下に起つて居ると云ふことは、非常に面白いことと思ふ。